energies

MDPI

Article

Flying a Micro-Drone by Dynamic Charging for Vertical Direction Using Optical Wireless Power Transmission

Tomoya Watamura, Takuo Nagasaka, Yuto Kikuchi and Tomoyuki Miyamoto *

Laboratory for Future Interdisciplinary Research of Science and Technology (FIRST), Institute of Integrated Research (IIR), Institute of Science Tokyo, R2-39, 4259 Nagatsuta, Midori-Ku, Yokohama 226-8503, Japan; watamura.t.aa@m.titech.ac.jp (T.W.); nagasaka.t.ab@m.titech.ac.jp (T.N.); yutoclimbing@gmail.com (Y.K.)
* Correspondence: tmiyamot@pi.titech.ac.jp; Tel.: +81-45-924-5059

Abstract: Micro-drones weighing less than about 200 g have a limited flight time of 5–15 min. Dynamic charging by optical wireless power transmission is a promising solution to this problem. This paper investigated the configuration and conditions required for dynamic charging of micro-drones by optical wireless power transmission and clarified the effect of weight change on the power required for flight and the size of solar cells that can be installed. Furthermore, a micro-drone equipped with a solar cell without a battery was used to demonstrate a vertical flight height of 75 cm at 35 W light output. The results are useful for continuous flight of micro-drones by optical wireless power transmission.

Keywords: optical wireless power transmission; laser; solar cell; drone; lens system; dynamic charging

1. Introduction

Drones are unmanned aerial vehicles (UAVs) that can fly freely in three-dimensional space and are used in a variety of applications, including aerial photography, delivering, sensing, agriculture, and entertainment [1,2]. There are two types of UAVs: the fixed-wing type, such as airplanes, and the rotary-wing type, such as helicopters. Since rotary-wing drones are attractive in a wide range of applications because they do not require a long runway and can hover, making them excellent for use in small spaces, this study focuses on the rotary-wing type, particularly motor-driven UAVs powered by electricity, which will be referred to as 'drones' in this paper. Among drones, micro-drones, whose weight is 200 g or less, are extremely attractive. Although the small size limits the delivery of heavy objects, it is possible to use small sensors and lighting devices, and this type is expected to have a very wide range of applications. In order to expand the applications of this micro-drone, it is necessary to remove the limitations associated with its small size.

The problem with these promising small drones is that their continuous flight time is extremely short, ranging from 5 to 40 min, depending on their weight. The flight time constraint also limits the flight distance. In particular, the flight time of micro-drones, which are expected to be used in a wide range of applications, is especially shorter, making it a major problem.

An attractive solution to this problem is dynamic charging by wireless power transmission [3]. This would allow for longer and, ideally, continuous flight and would also eliminate or greatly reduce the need for on-board batteries. Wireless power transmission for drones or airplanes has been investigated using electromagnetic induction and microwave systems [4–7]. However, electromagnetic induction is limited to very short transmission distances of less than few tens of centimeters; dynamic charging is difficult. Microwave

Academic Editor: Tek Tjing Lie

Received: 15 December 2024
Revised: 29 December 2024
Accepted: 13 January 2025
Published: 15 January 2025

Citation: Watamura, T.; Nagasaka, T.; Kikuchi, Y.; Miyamoto, T. Flying a Micro-Drone by Dynamic Charging for Vertical Direction Using Optical Wireless Power Transmission. *Energies* **2025**, *18*, 351. https://doi.org/10.3390/en18020351

systems can supply power over long distances, and there is a flight demonstration of a large drone (>2 kg) [5], but their long wavelengths result in large beam divergence, which reduce the beam collection rate over long distances, or require larger antennas on the transmitter and receiver sides, which pose challenges for application to micro-drones with high energy efficiency. Larger antennas may increase the weight and power consumption of micro-drones. In addition, these existing wireless power transmission methods use high-power AC or high-frequency radio waves, which can cause electromagnetic noise interference with other devices.

Optical wireless power transmission (OWPT) [8], which is based on a beam light source and a light-receiving device, is a promising new wireless power transmission method. Due to the short wavelength of light, OWPT can supply power over long distances with high beam collection rate even in compact configurations and has the advantage of being free from electromagnetic noise interference with other devices. Therefore, OWPT is suitable for dynamic charging to micro-drones.

Based on the above background, the purpose of this study is to clarify the necessary configuration and conditions for realizing dynamic charging to micro-drones by OWPT and to realize flight of micro-drones equipped with solar cells. Parts of the results shown in this study were presented in the fourth Optical Wireless Power Transmission Conference (OWPT2022), fifth Optical Wireless Power Transmission Conference (OWPT2023), and twenty-eighth Microoptics Conference (MOC2023) [9–11]. In this study, the comprehensive characteristics of drones, the detail of experimental conditions, and the improvement result of the flight experiment are additionally discussed.

This paper is organized as follows: Section 2 summarizes the flight time, weight, and other conditions of commercial drones and clarifies the issues in detail. In Section 3, the power required for flight of the micro-drone was evaluated, and the flight condition was clarified using the power by OWPT under the condition that the micro-drone is wired by a solar cell installed on the ground. In Section 4, the effect of installing solar cells on the micro-drone on its flight is experimentally evaluated. In Section 5, the vertical flight of a micro-drone equipped with solar cells by OWPT is demonstrated, and based on the characteristics of the light source and lens, the experimental results with increased flight height are shown. Finally, Section 6 summarizes the results and presents conclusions.

2. Current Status of Drones

2.1. Relationship Between Weight and Flight Time of Commercialized Drones

Drones have been used in a variety of industrial applications since mid-2010. Advances in motor, sensor, and control technology have led to the development and improvement of drones of different sizes for different purposes. Among them, micro-drones weighing less than about 200 g are particularly important. Both the body itself, which is compact and lightweight, and continued improvement of small high-resolution cameras and powerful sensors enable sufficient performance in aerial photography and inspection despite their small size. They have various applications, such as crop inspection [12] and surveying [13]. In addition, for drone shows that use a large number of drones to create three-dimensional images in space, micro-drones are of sufficient size because the only additional equipment is a visible light source. Such micro-drones are unlikely to cause damage to people or objects in the event of a crash or collision [14]. Therefore, they are generally easy to operate within flight regulations; although, these may vary by country [15].

However, one major challenge for drones, particularly micro-drones, is their limited continuous flight time. Figure 1 shows the recent relationship between the nominal weight (including battery) and flight time for many commercialized drones. The data source for the specifications of the drones is listed in Supplementary Materials Table S1. Figure 2

shows the ratio of the installed battery weight to the nominal weight (including battery), assuming a typical energy density of 200 Wh/kg for the battery capacity specification of a Li-ion polymer battery.

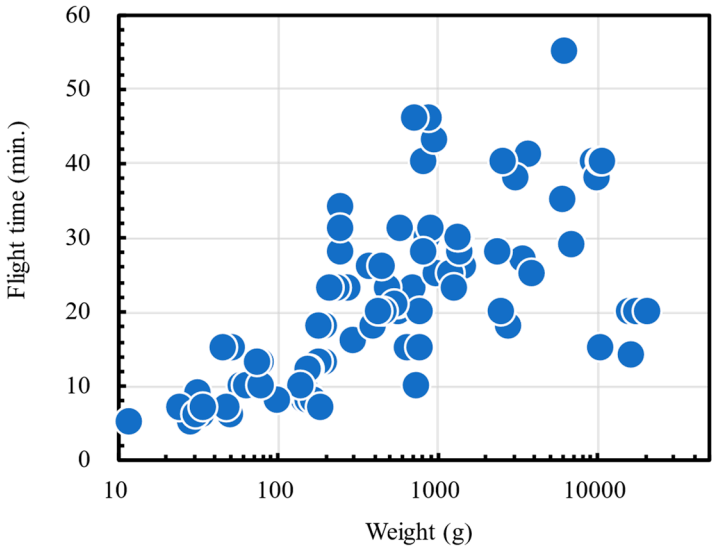

Figure 1. Relationship between the weight and flight time of commercial drones.

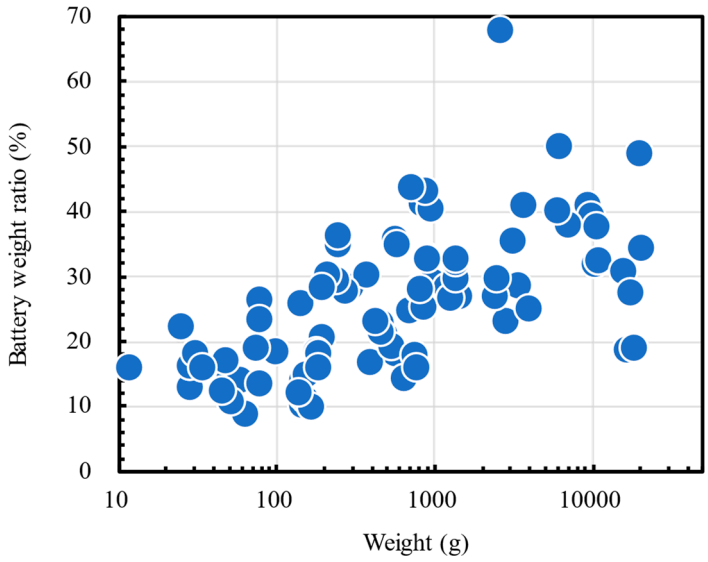

Figure 2. Relationship between weight and ratio of the battery weight of commercial drones.

Figure 1 shows that the maximum continuous flight time is less than about 40 min, regardless of the size of the drone. This is due to the fact that the weight of the on-board battery accounts for 20–50% of the total weight of the drone. Even if additional batteries are installed to extend the flight time, the flight time cannot be extended because power is consumed to transport the additional batteries. In addition, micro-drones weighing less than 200 g have a very short flight time of about 5–15 min. This is because it is difficult to reduce the non-battery weight ratio, such as the weight ratio of the motor, chassis, and electric circuit, to the total weight compared to larger drones, and the battery weight ratio is small, as shown in Figure 2.

Some drones are equipped with low-power cameras and sensors that do not significantly affect the flight time, but other applications, for example, drone shows, use high-brightness LEDs with a light output of several watts or more, which severely limits

the flight time due to large power consumption, and the show time is typically no longer than about 4–5 min.

Furthermore, the use of batteries in drones also requires them to be replaced and recharged, and the inability to fly while the batteries are being replaced is also a problem and limitation for expanding the variety of applications. The preparation of spare drones and spare batteries, as well as the work required to handle the batteries, is especially problematic when many drones are used, such as in a drone show.

Therefore, it is important to develop a technology that can solve this problem and enable continuous flight.

2.2. Previous Report of Dynamic Charging to Drones by OWPT

Therefore, it is necessary to realize dynamic charging to drones using OWPT. The OWPT field has been actively researched and developed in recent years. Various efforts have been made to improve the characteristics of light receiving device for OWPT [16–18], to theoretically optimize an OWPT dynamic charging system for drones [19,20], and to study the components of the system [21–26].

However, there have only been four cases of actual flight demonstrations of drones by OWPT. These cases are limited to relatively mid-sized or large drones weighing from a few 100 g to 1 kg [27–31]. For micro-drones weighing less than 200 g, there have been cases of about a 7% increase in flight time using additional power by OWPT while using batteries [32], but there are no reports of flights only by the power from OWPT.

When the size of the drone is large and heavy, the increased light output of the light source is a limiting factor in system realization, but various functions, including the receiver system for OWPT, can be easily installed on the drone, which leads to an increase in feasibility. On the other hand, small drones are likely to be subject to various limitations in the installation of functions for OWPT, as well as limitations in the amount of installed battery energy. Therefore, it is important to experimentally clarify the configuration and conditions necessary for dynamic charging to micro-drones by OWPT.

3. Evaluation of the Power Required for Flight of a Micro-Drone

3.1. Preparation of Micro-Drones

The micro-drone shown in Figure 3 (G-Force Inc., Tokyo, Japan, HUBSAN X4 HD) was used for the experiment to evaluate and demonstrate dynamic charging to micro-drones by OWPT. The size of the drone is as small as 120 mm square, including the 55 mm diameter propeller, and the weight of the battery is as small as 51 g. However, the maximum flight time with the battery is only 6 min in the specification. The micro-drones used are also included in Figures 1 and 2, and follow the general trend in commercialized drones.

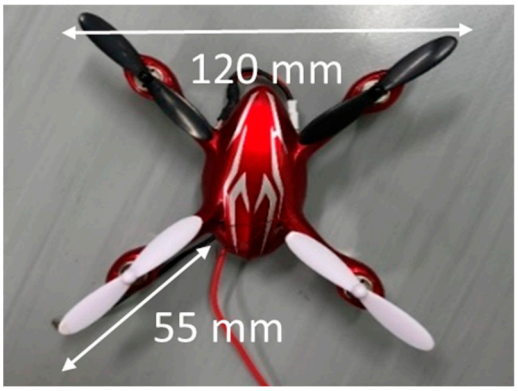

Figure 3. Micro-drone used in the experiment.

Figure 4 shows the relationship between the nominal weight (including battery) of a commercialized drone and its power consumption during flight. The power required for hovering of the drone, P_h, generally increases with weight M. This is because the rotation of the propeller must generate a thrust T equal to or greater than the gravitational force Mg acting on the drone. Here, g is the acceleration of gravity. Under the condition that $T = Mg$, which corresponds to hovering condition, the relationship is as shown in Equation (1) [33]:

$$P_h = \frac{T^{3/2}}{\eta_p \sqrt{2\rho A}} = \frac{(Mg)^{3/2}}{\eta_p \sqrt{2\rho A}} \quad (1)$$

where η_p is the propeller efficiency, A is the propeller area, and ρ is the air density. In this equation, power is proportional to the 3/2 power of weight, but the graph shows a power consumption relationship that is nearly proportional to weight due to the effect of changes in propeller area as a function of weight, that is, $P_h = 0.095(\mathrm{W/g}) \cdot M^{1.15}$.

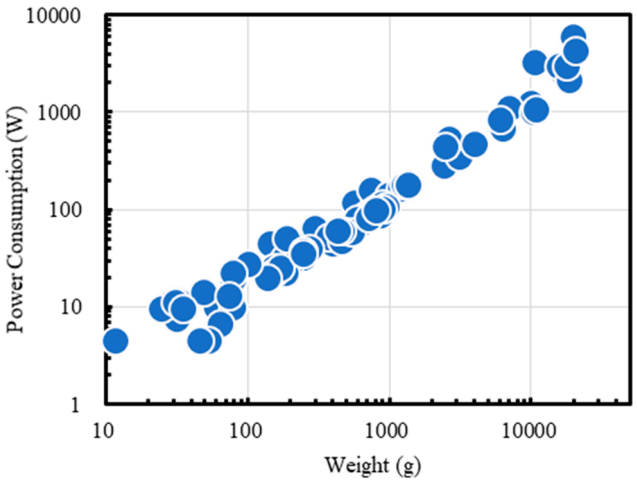

Figure 4. Relationship between weight and power consumption of commercial drones.

As a result, it is necessary to increase the amount of power supplied by OWPT and the light output of the light source as the weight of the drone increases. In this study, the required light output was suppressed by reducing the weight of the micro-drone as much as possible, taking into account the preparation of high-power laser sources and their safe handling in experiments. For this reason, the battery and charging circuits, which are ideally unnecessary for the OWPT system, were removed, and the flight control circuit was also removed by limiting the experiment to vertical flight. By eliminating these batteries and circuits, the drone weight was reduced to 34.5 g, 68% of the product specification of 51 g. In addition, this study also did not use the MPPT (Maximum Power Point Tracking) circuit [34,35], which operates the solar cell output at maximum efficiency through impedance tracking control, which is commonly used in solar power generation as the initial evaluation.

The reason for limiting the experiment to vertical flight is explained here. Note that when moving a drone, a large amount of energy is required to move vertically, but less energy is required to move parallel to the ground. For dynamic charging during three-dimensional free flight, the drone scans a light beam by detecting the solar cells mounted on the drone, and this beam-tracking system is an additional function of the light source side based on existing technology. In contrast, to supply power, the main function of optical wireless power transmission is closely related to the configuration and characteristics of the light-receiving side (drone), such as the configuration and conditions of the light-receiving device and the amount of the power supplied to the drone. Therefore, if vertical flight can

be realized by OWPT dynamic charging, it will be easy to expand to three-dimensional free flight. In addition, even under the limitation of vertical flight, drones can be used in a variety of applications, such as hovering at a fixed position or changing only in one direction, such as the Z-axis direction. For this reason, only vertical flight is considered in this study. In some previous reports of OWPT dynamic charging for relatively large drones, dynamic charging during three-dimensional free flight has also been demonstrated using a beam-tracking system. The ability to easily install additional functions due to the large size and weight of the drone is also thought to have been effective.

3.2. Evaluation of the Effect of Weight on Power Required for Flight

The micro-drones need to be additionally equipped with solar cells and other devices for OWPT. For this purpose, the effect of the weight change in the prepared drone on the power consumption was evaluated in detail.

The power required for flight of the lightweight micro-drone was evaluated by wiring the drone's motor and DC power source. The drone will continue to rise if a power greater than the power P_h shown in Equation (1) is supplied within the range where the atmospheric pressure can be assumed to be constant. However, in this experiment, wires are connected to the drone, and as the drone rises, the weight of the wires suspending the drone increases, causing the drone to stop rising at a certain height. Under these conditions, weights of 1 g each were added to the micro-drones in turn, and the output of the DC power source was controlled so that the flight height was a constant value of 20 cm.

Figure 5 shows the relationship between the power and the weight of the added weights, including the effect of the 2 g weight on the wires for 20 cm. The dotted line is the result of the analysis based on Equation (1) for the no weight case, taking into account the drone weight, wire weight, and added weight.

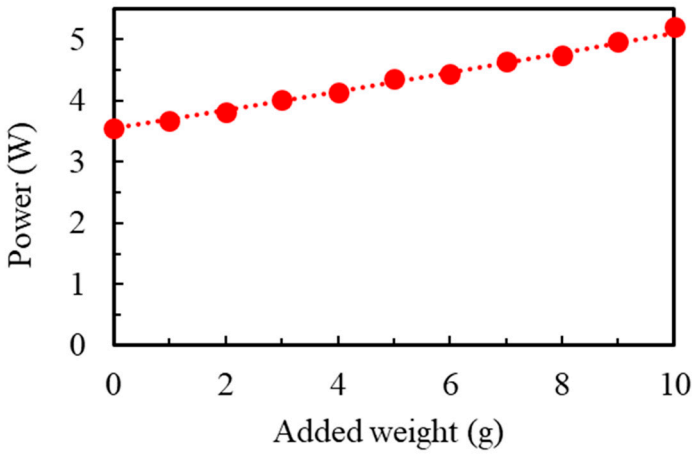

Figure 5. Variation in power required for flight with respect to added weight. The red plot: measurement value, the dotted line: estimated value based on Equation (1).

The graph shows a good agreement with the power required for flight vs. weight based on Equation (1), which is shown by the dotted line. Therefore, even a few grams, which is about 10% of the weight of a micro-drone, requires a 10% increase in the required power. It can be said that considering the weight in units of 1 g is important for the installation of solar cells for OWPT in micro-drones.

3.3. Flight Powered by Ground-Mounted Solar Cells

After determining the relationship between the weight of the micro-drone and the power consumption during flight, the next step was to evaluate the flight conditions for powering by OWPT. In this section, the solar cell module was installed on the ground

and wired from the solar cell to the drone. The experiment of this Section was conducted to confirm that flight was possible using only OWPT power. In other words, flight was confirmed using power generated by solar cells irradiated with laser light.

A surface-emitting laser (VCSEL) array (Princton Optronics Inc., Trenton, NJ, USA, PCW-CA1-40-W0808) was used as the light source, which can emit a high-power light beam with uniform intensity in a two-dimensional array. The VCSEL array chip has an emitting area of 5 mm square, a maximum light output of 40 W, and a wavelength of 808 nm. This VCSEL array was used for all light sources in this paper. Light source conversion efficiency was 22% at 30 W light output.

On the light-receiving side of OWPT, it is important to irradiate the entire rectangular solar cell module with a uniform intensity light beam [36], and a rectangular VCSEL array is advantageous because, in general photovoltaic power generation, a series connection of multiple solar cells is used to increase the output voltage. Since each element in the VCSEL array emits circular beams at some divergence, the overlapping of individual beams would result in a circular irradiation pattern with high central intensity without lens, causing light leakage from the solar cell by mismatch of the shape and reduced efficiency due to ununiform intensity irradiation. In addition, an ideal collimated beam cannot be generated because it is not a point light source. Therefore, the method where the square emitting area of the VCSEL array is enlarged and projected onto the solar cell according to the imaging conditions of the lens is a good candidate.

Solar cell selection for OWPT drones depends on conversion efficiency and power per weight under monochromatic, high-intensity irradiation. GaAs outperforms Si because its direct bandgap allows for thinner, lighter, and more flexible cells. Recently, advanced perovskites could match the performance of GaAs while being cheaper and lighter, but they have been minimally evaluated under monochromatic, high-intensity conditions. Currently, perovskite cells have higher series resistance losses that reduce efficiency compared to GaAs [37]. Further advances in perovskite cells will make them more viable for OWPT applications.

For the solar cell modules, flexible GaAs solar cells with high photoelectric conversion efficiency, thinness, light weight, and deformability were used because the weight of a few grams affects the flight characteristics, as described in the previous section. A GaAs solar cell module (manufactured by Advanced Technology Institute, LLC., Tokyo, Japan) with a size of 5 cm $\times$ 8 cm, consisting of five cells in series, and a module weight of 1.8 g was used. The open-circuit voltage under solar irradiation is 5.5 V, and the photoelectric conversion efficiency is about 20%. It is notable that the photoelectric conversion efficiency is higher than that of sunlight because a monochromatic light source is used in OWPT instead of sunlight. The 808 nm (1.53 eV) wavelength of the VCSEL is close to the optimum for the bandgap energy (1.42 eV) of the GaAs. The two GaAs solar modules were connected in parallel in a V-shape to form a square with an effective shape of 8 cm squares. The V-shape is defined by the condition that the fold in the center of the V-shape is close to the light source. The square shape beam from the VCSEL was irradiated onto the solar modules and enlarged by a lens.

The current–voltage (IV) characteristics of the solar cell during this light beam irradiation are shown in Figure 6. The graph also shows the operating point of the micro-drone without flight control circuit and battery at the start of flight by the power of a DC power source. A straight line shows the I-V characteristic, assuming that the drone has a linear load resistance passing through this point.

It was confirmed that the I-V characteristics of the solar cell with a VCSEL light output of 15.9 W exceeded the conditions at the start of flight.

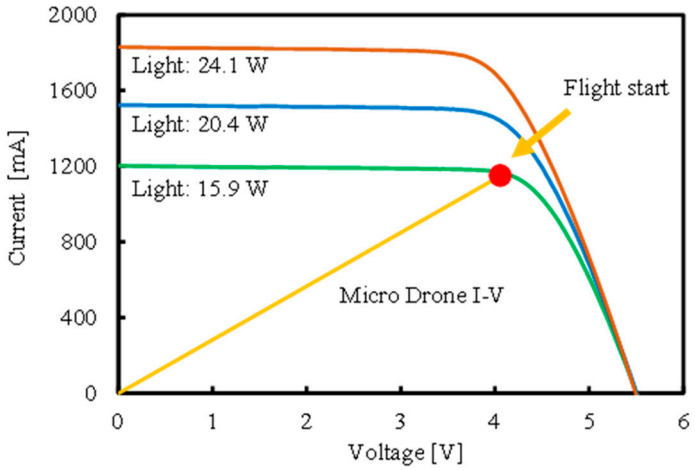

Figure 6. IV characteristics of solar modules connected in parallel.

Figure 7 shows the flying of the micro-drone when the solar cells were irradiated with 24.4 W of light. It was confirmed that the drone could fly up and stop to rise at a height of 64 cm under wiring condition from ground-mounted solar cells. From Equation (1), the power required for flight at this height is about 30% higher than at the start of flying (height: 0 cm) because the drone suspends wire weight of approximately 6 g (20% of the body weight). Thus, when flying with wires, flight height is limited as a function of the supplied power and the height determined by the weight of the wires.

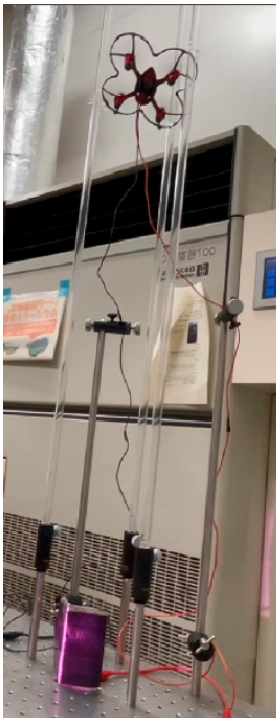

Figure 7. OWPT to ground-mounted solar cells (24.4 W light output).

4. Evaluation of Solar-Cell-Mounting Conditions

4.1. Evaluation of Mountable Solar Cell Sizes

Next, mounting the solar cells on the micro-drone was investigated. In an author's previous initial experiment, the solar cell was suspended vertically from the micro-drone and irradiated with light from directly beside the solar cells to confirm that it could fly up to 1–2 cm height by OWPT [38]. In this case, since the light beam scanning was not applied,

the beam irradiation position to the solar cell was fixed, and the flight height was limited to 1–2 cm. In this paper, to enable a higher flight height, the solar cells are suspended parallel to the ground from a micro-drone, and the light is irradiated from directly below the solar cells.

In this configuration, the airflow generated by the propeller hits the solar cells, reducing the thrust. To evaluate this effect, as shown in Figure 8, a square plate with sides ranging from 30 mm to 120 mm in length was suspended directly below the drone to simulate a solar cell, and the effect on the drone's thrust was evaluated in terms of changes in power required for flight. It was supplied by a DC power source. The weight of the square plate was set to 8.4 g for all plate sizes.

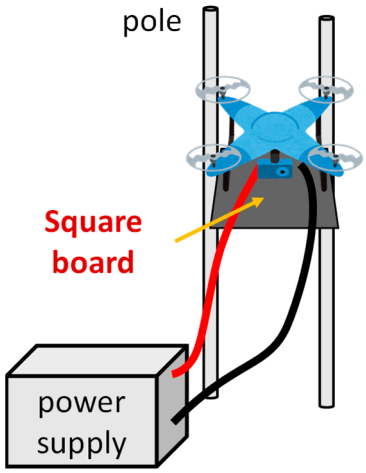

Figure 8. Experimental configuration for evaluation of solar cell mountable size.

The results are shown in Figure 9. S_p and S_o are the area of the rotating surface of the propeller and the area where the square plate and the propeller overlap, respectively. The vertical axis is the power at the beginning of the flight. The results show that when the airflow of the propeller is obstructed by the solar cells, the required power is several times higher than that without the plates. Flight was impossible when the cover ratio of S_o/S_p was greater than 0.9. The size of the solar cells actually mounted on the drone must be taken into account in terms of the amount of power generated, the amount of heat generated, and other factors, as well as the size and weight limitations of the solar cells available. In order to suppress the influence on flight characteristics, the cover ratio must be 0.2 or less, and in order to have a sufficiently small influence, it is important that the cover ratio is 0.1 or less.

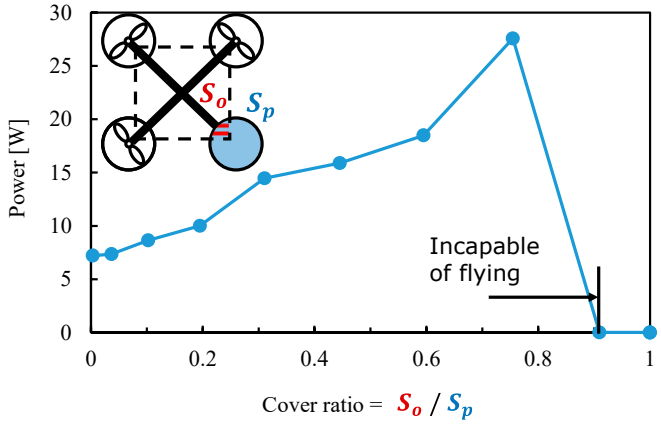

Figure 9. Variation in power at the start of flight with respect to shielding of the propeller rotation area.

4.2. Comparison of Solar Cell Mounting Method

From the previous Section, the effective area of the solar cells must be small enough for the size of the drone. The solar cell module prepared for this study is rectangular, and its size is too large in the case of the configuration described in Section 3.3., which consists of two modules. For this reason, a single module was used for mounting. Since the light beam shape is assumed to be square, the effective size was reduced to 50 mm × 50 mm by mounting the solar cells in two ways: diagonal mounting and inverted U-shape mounting, as shown in Figure 10. In this case, the cover ratio in Figure 9 is 0.1, which is sufficiently small. The inverted U-shape was possible because the GaAs solar cells used in this study are flexible type. The weight of a drone without the battery, without the control circuit, and with the solar cell module is 37.1 g.

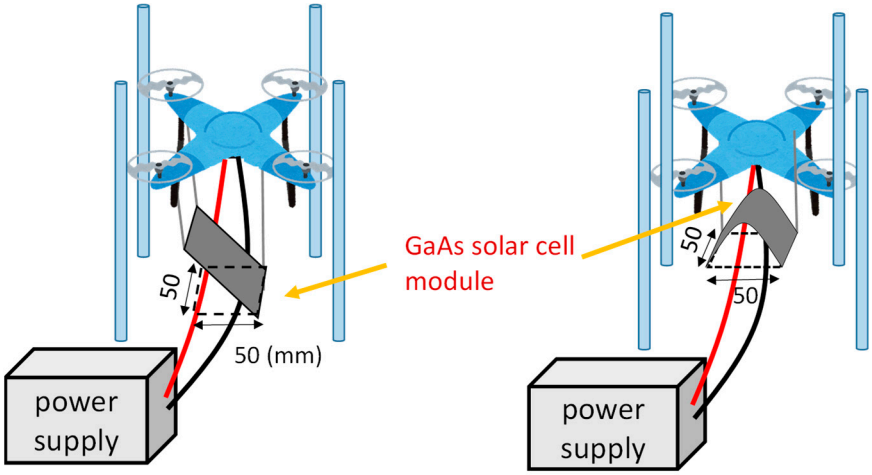

Figure 10. Experimental configuration for comparison of solar-cell-mounting conditions (**left**: diagonal mounting, **right**: inverted U-shape mounting).

Figure 11 shows the drone powered by a DC power source, before and after the start of flight, with the GaAs solar cells mounted diagonally and in an inverted U-shape.

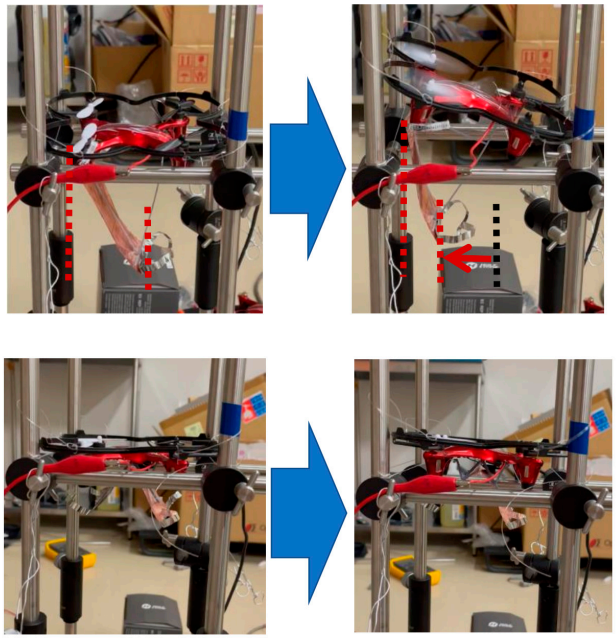

Figure 11. Comparison of solar-cell-mounting method (**top**: diagonal, **bottom**: inverted U-shape).

The results show that when the GaAs solar cells were mounted diagonally, the center of gravity of the drone shifted from the center of the fuselage due to the wind generated by the propeller, causing the flight posture to tilt. This resulted in a decrease in the effective light-receiving area and unstable operation due to oscillations in the tilt of the solar cells. In contrast, the inverted U-shaped mount remained nearly horizontal flight posture. Therefore, it was confirmed that it is necessary to mount solar cells that can equalize the influence of the propeller airflow.

4.3. Characterization of Solar Cells Mounted on the Micro-Drone

The I-V characteristics of the solar cells were evaluated while mounted in an inverted U-shape on the micro-drone. The results are shown in Figure 12. The operating point at the start of flight and the load I-V characteristics of the drone equipped with solar cells evaluated using a DC power source are also shown.

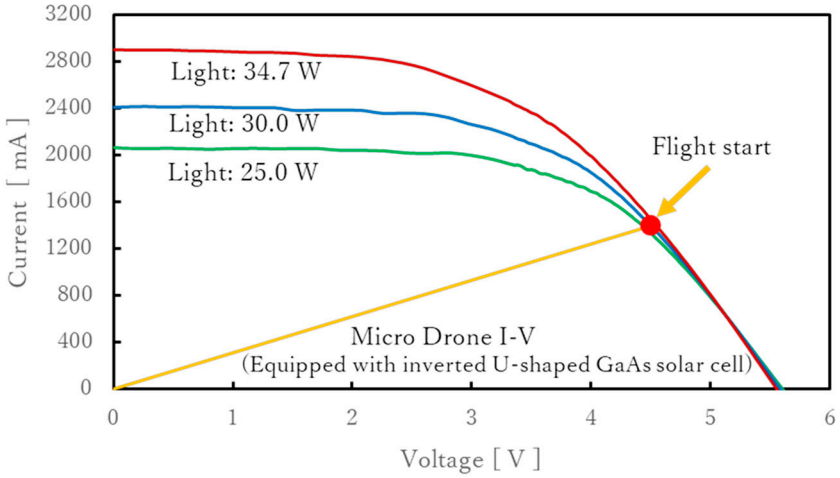

Figure 12. Evaluation I-V Characteristic of Inverted U-Shaped Solar Cells.

The evaluation of two GaAs solar cell modules connected in a V-shape shown in Figure 6 can be interpreted the same characteristics as a single module; although, there is a difference in light intensity density due to the parallel connection. Comparing Figures 6 and 12, there was no deterioration in the I-V characteristics when the modules were connected in an inverted U-shape, but the short-circuit current increased by about 10% for the same light output in an inverted U-shape. The cause of this increase is not yet understood, but it is believed to be due to increased light absorption caused by multiple reflections on the solar cell surface due to the inverted U-shape.

Figure 13 shows the conversion efficiency at the optimal operating point of the inverted U-shaped solar cell and the actual operating point, i.e., the intersection with drone IV. From Figure 13, it can be seen that the operating efficiency is lower than the optimal conversion efficiency except for a specific light output. To avoid this effect, the MPPT circuit can be utilized to operate at the optimum operating point regardless of the light output. On the other hand, it should be noted that the additional circuit increases the drone power consumption and weight.

As a result, it was found that the micro-drone could fly with 25 W light output or more. The reason for the higher required light output compared to the flight conditions shown in Section 3.3 is the increase in weight due to the mounting of the solar cells and the effect of the solar cells on the airflow.

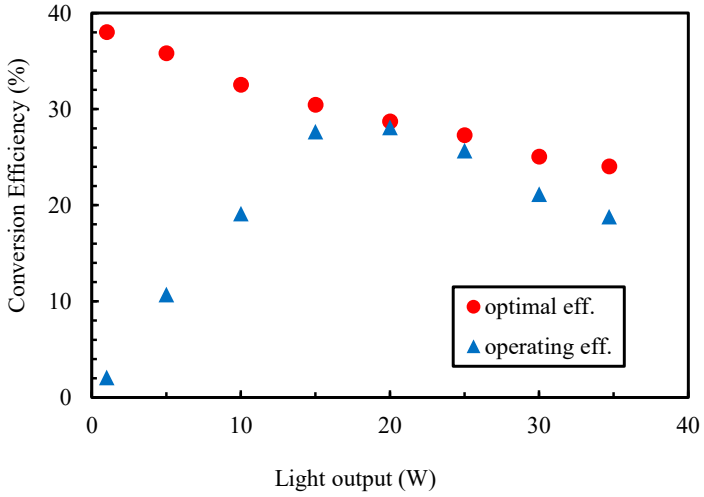

Figure 13. Comparison of operating efficiency and optimal efficiency.

5. Vertical Flight Demonstration of a Micro-Drone Equipped with Solar Cells

5.1. Experimental Configuration

A flight experiment was conducted with GaAs solar cells mounted in an inverted U-shape. The weight of a drone without the battery, without the control circuit, and with a solar cell module, is again 37.1 g. The experimental configuration is shown in Figure 14. The flight range of the drone was limited to the vertical direction, and the VCSEL light source was positioned directly under it with a lens (focal length: f = 20 mm) so that the beam size at the standby position of the micro-drone was approximately 50 mm square.

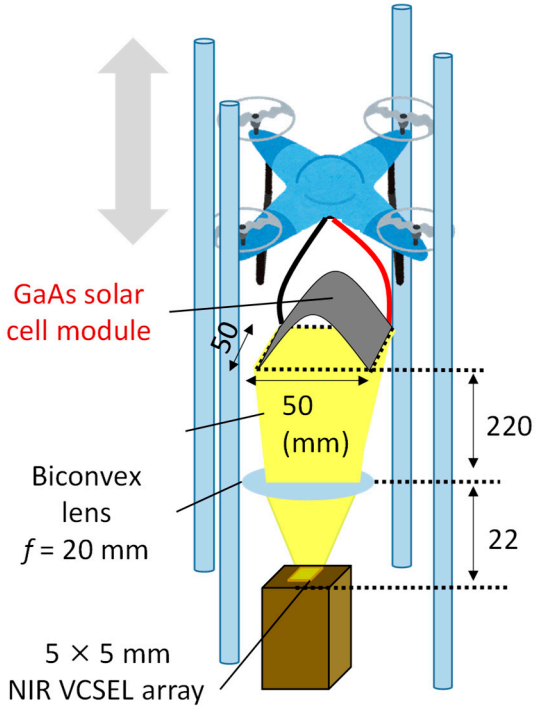

Figure 14. Experimental configuration for vertical flight of micro-drone.

Curvature of the inverted U-shape solar cells usually does not degrade the efficiency of flexible solar cells, although uniform light absorption and avoidance of curvature-induced breakage are important. Optimal performance requires uniform irradiation for

cells connected in series. The applied condition in this study is that the efficiency is slightly degraded from the flat condition due to slight non-uniform irradiation.

5.2. Experiment Results

When irradiated with a VCSEL light output of 23.5 W, the drone flew up and stopped rising at a height of 3 cm from standby position, and when irradiated with a light output of 30 W, it flew up to a height of 7 cm as shown in Figure 15. The micro-drone continued to fly stably as long as the light beam was irradiated.

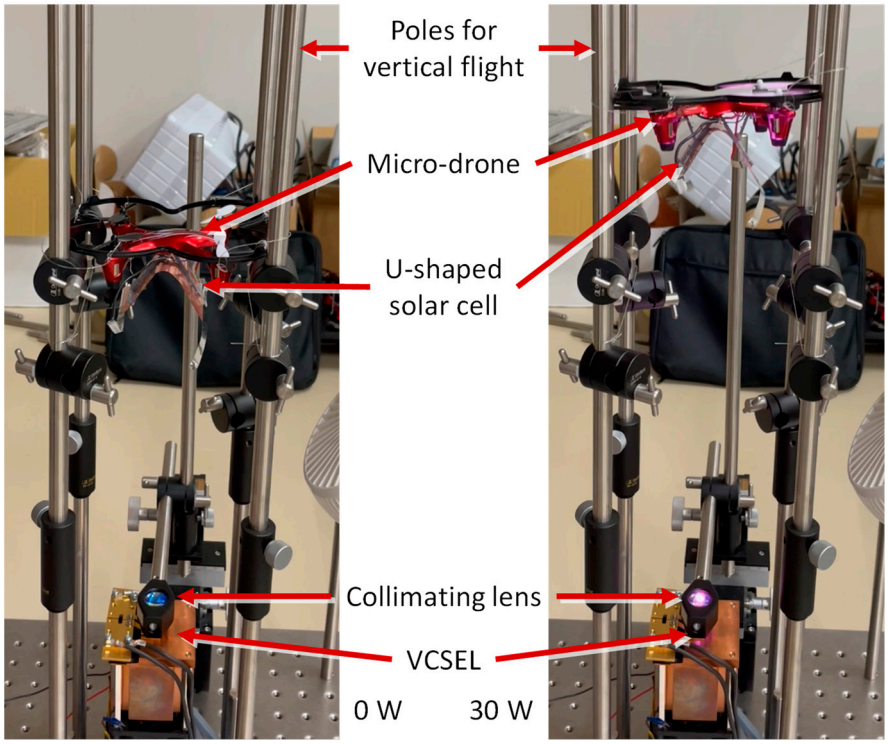

Figure 15. Vertical flight demonstration of micro-drone.

5.3. Effect of Lens Configuration on Flight Height

As described in Section 3.1, if the propeller thrust exceeds the drone weight, the drone can continue to increase its flight height as long as the air density does not change. However, in the experiment described in the previous Section, the drone was flying stably, and its height was almost fixed as a function of the light output. This is believed to be due to beam divergence. It causes light leakage in proportion to height and the decrease in the power supplied to the drone as it rises. Thus, thrust and weight balance at a certain height, and the drone stops rising.

In addition to beam divergence, with a fixed-lens system, changes in the irradiation height cause defocus before and after the focus position. In this experiment, the focus position was set at the standby position of the drone (Z = 0), as shown in Figure 14. Therefore, it is believed that the amount of light which the solar cell module receives and the power generated by the solar cells decreased as the flight height increased due to beam divergence and defocus.

To evaluate the effect of beam characteristics, three lens configurations (f = 20 mm, 70 mm, 200 mm) were prepared as shown in Figure 16, with the conditions shown in

the figure based on the VCSEL array size, standby position, and solar cell size. In these configurations, the following lens formula was used:

$$\frac{1}{f} = \frac{1}{a} + \frac{1}{b} \tag{2}$$

$$m = \frac{b}{a} \tag{3}$$

where a is distance between the VCSEL chip and the lens, b is distance between the lens and target object, and m is magnification.

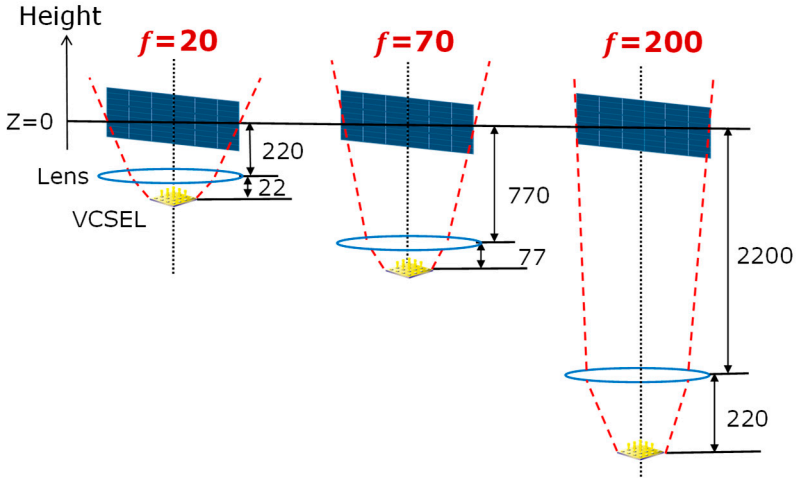

Figure 16. Comparison of lens configurations (unit: mm).

The beam size was measured at each height (distance) using an infrared viewer (ElectroViewer 7215, Electrophysics Inc., Fairfield, NJ, USA) The beam size was measured visually by projecting the beam onto a sheet of graph paper, as the measurement error due to defocus was considered to be small in the measurement range ($0 < Z < 20$ cm at f = 20, 70 mm, and $0 < Z < 50$ cm at f = 200 mm). The evaluation results are shown in Figure 17. The vertical axis is the ratio of the amount of the light output which the solar cell module receives to the light output of the light source, and the horizontal axis is the height from the standby position. The markers indicate the measurement results, and the dotted line is the calculation result assuming a linear variation of the beam size with distance. Figure 17 shows that applying the lens with a longer focal length reduces the beam divergence and suppresses light leakage to higher positions.

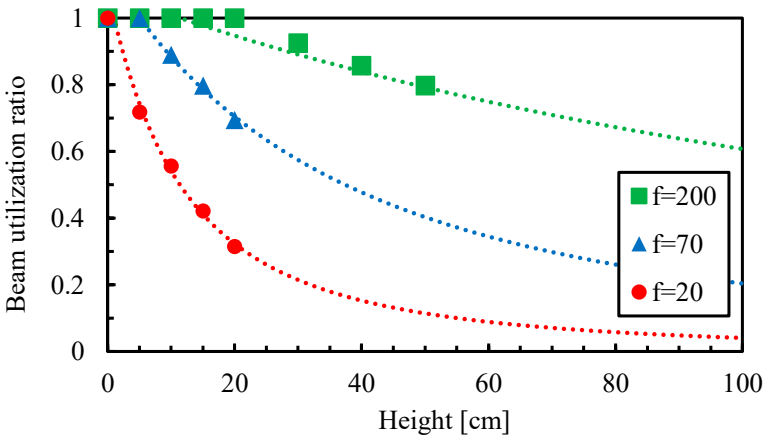

Figure 17. Variation in beam utilization ratio as a function of height from the focused position.

Based on the above results, using a lens of f = 70 mm, a flight experiment was conducted, and it was confirmed that the drone flew up to a height of 25 cm at 30 W light output and a height of 35 cm at 35 W light output, as shown in Figure 18.

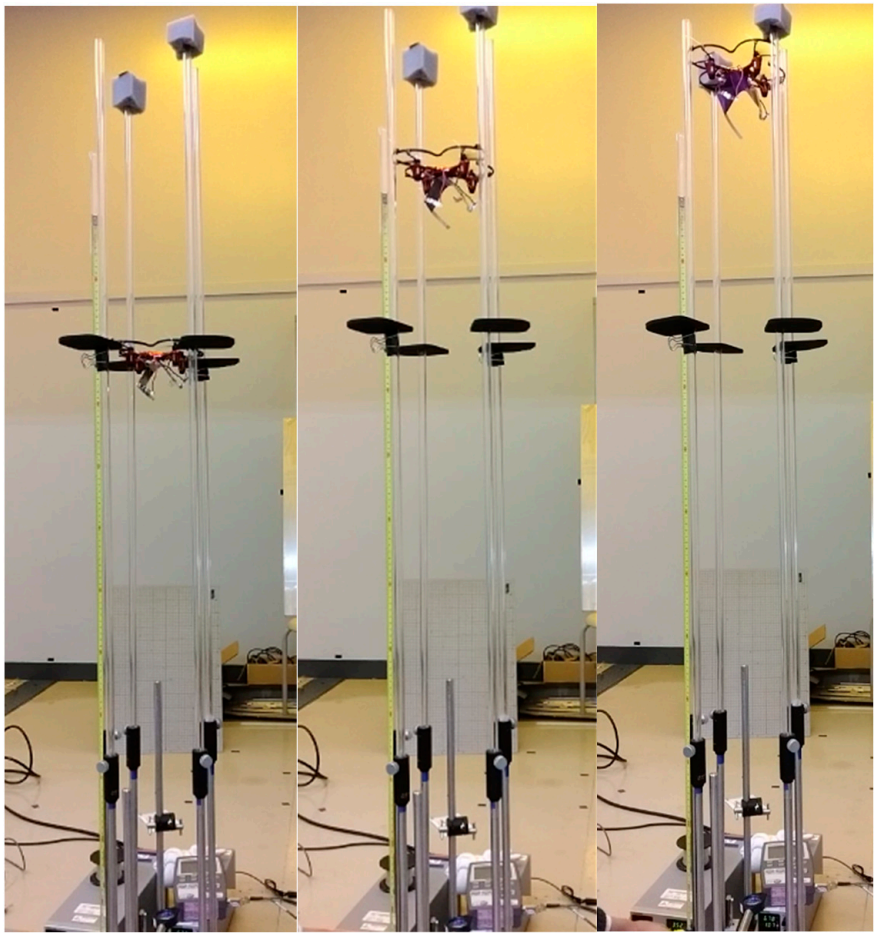

Figure 18. Higher flight by lens replacement (from left to right: 0 W, 30 W, and 35 W light output).

Based on these results, it is inferred that the drone will fly up to a height where the beam utilization ratio is about 0.5 in Figure 17 at a 35 W light output, so it is expected that the drone is able to fly up to a height of more than 100 cm with a lens of f = 200 mm. Therefore, an experiment with a lens of f = 200 mm was conducted, as shown in Figure 19 (Video S1, Supplementary Materials) and achieved flight up to 75 cm height with 35 W light output.

Table 1 summarizes the results of the micro-drone flight experiments. It was confirmed that the use of a long focal length lens can suppress light leakage in wide range and enable higher flight. In this method, the longer the focal length, the larger the lens diameter must be to suppress vignetting losses at the lens due to the beam spread of the light source. In addition, even if the focal length is increased, the beam spread increases depending on the size of the light source. This, in turn, limits the distance at which power can be supplied. In addition, if the drone and the light source are not facing each other, the beam shape will be deformed, and the application of another beam shape control technology will be necessary. In the future, it will be possible to achieve higher flight by increasing the light output or by using zoom optics to optimize the beam shape and beam size at an arbitrary position, even at constant light output.

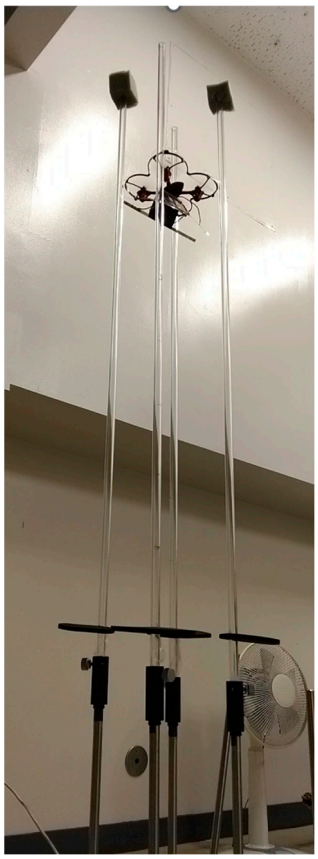

Figure 19. Higher flight with updated lens (35 W light output).

Table 1. Experimental results of micro-drone vertical flight.

Focal Length of Lens (mm)	Light Output (W)	Flight Height (cm)
20	23.5	3
	30	7
70	30	25
	35	35
200	35	75

The overall system efficiency is expressed as the product of the light source conversion efficiency, the solar cell conversion efficiency, and the beam utilization ratio. From Figure 17 and Table 1, it is estimated that the solar cells on the drone while floating receive approximately 18 W light. The conversion efficiency and output from solar cell are estimated to be 28% and 5 W, respectively, from Figure 13. As a result, the overall system efficiency during the floating was about 4%. System efficiency is constrained by the conversion efficiency of the devices, and further research is expected. For example, there are reported cases of devices exceeding 70% in light sources [39]. In addition, solar cells designed for OWPT (laser power converters) have reported photoelectric conversion efficiencies of up to 69% [40]. By combining these devices and adjusting the irradiation conditions, the overall efficiency will be increased to about 50%.

In addition to flight height extension, to demonstrate the effectiveness of an optical wireless power transmission in addressing the crucial problem of flight time limitation, a 60 min irradiation experiment was conducted at 30 W light output. As a result, it was confirmed that the micro-drone flew stably for the duration of the irradiation, attaining a flight time of 60 min, that was not possible with current battery specification.

Table 2 compares the configuration and characteristics of the OWPT system in this study with those of other cases that have demonstrated OWPT dynamic charging to the drones. In this work, a quite small and light weight drone was demonstrated. These studies extended that the OWPT can be applied to a wide range of weights.

Table 2. Comparison of OWPT systems for dynamic charging to drone.

Reference	Kinki Univ. (2008) [27]	Powerlight Inc. (2010) [28,29]	Naval Research Lab. (2014) [30]	Northwestern Polytechnical Univ. (2023) [31]	This Work
Size	60 cm sq. *	50 cm sq.*	50 cm sq *	30 cm sq. *	12 cm sq.
Solar cell Size	30 cm φ	30 cm sq *	30 cm φ *	10 cm sq. *	5 cm sq.
Weight	1.2 kg	1.05 kg	1.7 kg	300 g *	37.1 g
Battery weight	40 g *	100 g	-	-	0 g
Light output	560 W	400 W *	2 kW	200 W *	23.5 W
Flight height/size (min/cm) (Flight height)	10 * (6 m *)	80 (40 m)	4 * (2 m *)	20 * (6 m *)	6 (75 cm)
Flight time/size (min/cm) (Flight time)	2 (2 h)	15 (12.5 h)	-	-	5.5 (60 min.)
Beam control optics	Collimator	-	Collimator	-	Imaging lens system

*: estimated from reference and typical relationship between drone size and weight, etc.

In addition, in this work, an imaging optical system that enables uniform illumination was used for beam control optics. Although the collimating beam allows the beam to propagate over long distances, the beam intensity distribution is non-uniform, so the arrangement of the solar cells should be optimized for efficient operation.

6. Conclusions

In this paper, the configuration for dynamic charging of micro-drones by OWPT was designed and experimentally verified. First, as an evaluation of the conditions required for dynamic charging to micro-drones by OWPT, the effects of the additional weight on the power required for the flight of the micro-drone without the flight control circuits and battery and the flight operation by OWPT using ground-mounted solar cells were confirmed. Next, the effect of the size and shape of the solar cells mounted on the micro-drone on the propeller airflow was evaluated, and the necessary size conditions were clarified. In addition, it was pointed out that a mounting method that can equalize the effect of the propeller airflow is effective for mounting the rectangular solar cells used in the experiments. Based on these results, the vertical flight demonstration of the micro-drone equipped with the solar cell was conducted. By adjusting the shape of the light beam, the drone was able to fly up to 75 cm with a light output of 35 W. The drone flew stably as long as the light beam was irradiated.

In conclusion, this study clarified the conditions required for dynamic charging of micro-drones by OWPT and demonstrated flight using only the power from OWPT. The results of this study, combined with target detection and beam-scanning technologies, will provide the basis for various future applications and developments, such as continuous flight, including free flight of micro-drones.

Supplementary Materials: The following supporting information can be downloaded at https://www.mdpi.com/article/10.3390/en18020351/s1: Table S1: Specification of commercial drones; Video S1: Vertical flight of a micro-drone.

Author Contributions: Conceptualization, T.M.; methodology, T.W. and Y.K.; formal analysis, T.N. and T.W.; investigation, T.N., T.W. and Y.K.; resources, T.M.; data curation, T.M.; writing—original draft preparation, T.W.; writing—review and editing, T.M.; visualization, T.W.; supervision, T.M.; project administration, T.M.; funding acquisition, T.M. All authors have read and agreed to the published version of the manuscript.

Funding: This work was partially supported by the Tsurugi-Photonics Foundation (No. 20220502) and based on results obtained from a project, JPNP14004, commissioned by the New Energy and Industrial Technology Development Organization (NEDO).

Data Availability Statement: Data are contained within the article or Supplementary Material.

Acknowledgments: We thank members of the T. Miyamoto Laboratory of Institute of Science Tokyo for discussion and assistance.

Conflicts of Interest: The authors declare no conflicts of interest.

References

1. Bogue, R. Beyond imaging: Drones for physical applications. *Ind. Robot* **2023**, *50*, 557–561. [CrossRef]
2. AL-Dosari, K.; Hunaiti, Z.; Balachandran, W. Systematic review on civilian drones in safety and security applications. *Drones* **2023**, *7*, 210. [CrossRef]
3. Mohsan, S.A.H.; Othman, N.Q.H.; Khan, M.A.; Amjad, H.; Żywiołek, J. A comprehensive review of micro UAV charging techniques. *Micromachines* **2022**, *13*, 977. [CrossRef] [PubMed]
4. Aldhaher, S.; Mitcheson, P.D.; Arteaga, J.M.; Kkelis, G.; Yates, D.C. Light-weight wireless power transmission for mid-air charging of drones. In Proceedings of the 11th European Conference on Antennas and Propagation, Paris, France, 19–24 March 2017; pp. 336–340. [CrossRef]
5. Brown, W.C. Experiments involving a microwave beam to power and position a helicopter. *IEEE Trans. Aerosp. Electron. Syst.* **1966**, *AES-5*, 692–702. [CrossRef]
6. Kaya, N.; Matsumoto, H. METS rocket experiment and MILAX airplane demonstration. *J. Space Technol. Sci.* **1992**, *8*, 16–21.
7. SHARP (Stationary High Altitude Relay Platform). Available online: https://www.friendsofcrc.ca/Projects/SHARP/sharp.html (accessed on 14 December 2024).
8. Miyamoto, T. Optical wireless power transmission using VCSELs. In Proceedings of the SPIE, Strasbourg, France, 22–26 April 2018; Volume 10682, p. 1068204. [CrossRef]
9. Kikuchi, Y.; Miyamoto, T. Design and characterization of dynamic OWPT charging to micro-drones. In Proceedings of the 4th Optical Wireless and Fiber Power Transmission Conference (OWPT2022), Yokohama, Japan, 18–21 April 2022. OWPT5-02.
10. Kikuchi, Y.; Watamura, T.; Miyamoto, T. Vertical flight demonstration of OWPT-based micro-drones with installed solar cells. In Proceedings of the 5th Optical Wireless and Fiber Power Transmission Conference (OWPT2023), Yokohama, Japan, 18–21 April 2023. OWPT10-02.
11. Watamura, T.; Miyamoto, T. Flight height extension of micro-drones by light beam shape control of optical wireless power transmission. In Proceedings of the 28th Microoptics Conference (MOC2023), Miyazaki, Japan, 24–27 September 2023. F-2. [CrossRef]
12. Itakura, K.; Noaki, S.; Hosoi, F. Fruit counting using autonomous flight of small UAV. *J. Jpn. Agric. Syst. Soc.* **2022**, *38*, 29–35. [CrossRef]
13. Pikalov, S.; Azaria, E.; Sonnenberg, S.; Ben-Moshe, B.; Azari, A. Vision-less sensing for autonomous micro-drones. *Sensors* **2021**, *21*, 5293. [CrossRef] [PubMed]
14. la Cour-Harbo, A. Mass threshold for 'harmless' drones. *Int. J. Micro Air Veh.* **2017**, *9*, 77–92. [CrossRef]
15. Lee, D.; Hess, D.J.; Heldeweg, M.A. Safety and privacy regulations for unmanned aerial vehicles: A multiple comparative analysis. *Technol. Soc.* **2022**, *71*, 102079. [CrossRef]
16. Fafard, S.; York, M.C.A.; Proulx, F.; Valdivia, C.E.; Wilkins, M.M.; Arès, R.; Aimez, V.; Hinzer, K.; Masson, D.P. Ultrahigh efficiencies in vertical epitaxial heterostructure architectures. *Appl. Phys. Lett.* **2016**, *108*, 071101. [CrossRef]
17. Helmers, H.; Höhn, O.; Lackner, D.; López, E.; Ruiz-Preciado, L.; Schauerte, M.; Siefer, G.; Dimroth, F.; Bett, A.W. Highly efficient III-V based photovoltaic laser power converter. In Proceedings of the 1st Optical Wireless and Fiber Power Transmission Conference, Yokohama, Japan, 23–25 April 2019. OWPT1-01.
18. Miyoshi, M.; Nakabayashi, T.; Yamamoto, K.; Dalapati, P.; Egawa, T. Improved epilayer qualities and electrical characteristics for GaInN multiple-quantum-well photovoltaic cells and their operation under artificial sunlight and monochromatic light illuminations. *AIP Adv.* **2021**, *11*, 095208. [CrossRef]

19. Ouyang, J.; Che, Y.; Xu, J.; Wu, K. Throughput maximization for laser-powered UAV wireless communication systems. In Proceedings of the IEEE International Conference on Communications Workshops, Kansas City, MO, USA, 20–24 May 2018; pp. 1–6. [CrossRef]
20. Jaafar, W.; Yanikomeroglu, H. Dynamics of laser-charged UAVs: A battery perspective. *IEEE Internet Things J.* **2021**, *8*, 10573–10582. [CrossRef]
21. Ying, J.; He, Y. UAV laser charging technology based on beacon laser alignment. In Proceedings of the SPIE, Hefei, China, 26–28 November 2018; Volume 11068, p. 1106809. [CrossRef]
22. Chen, Q.; Zhang, D.; Zhu, D.; Shi, Q.; Gu, J.; Ai, Y. Design and experiment for realization of laser wireless power transmission for small unmanned aerial vehicles. In Proceedings of the SPIE, Beijing, China, 5–7 May 2015; Volume 9671, pp. 133–139. [CrossRef]
23. William Setiawan Putra, A.; Kato, H.; Maruyama, T. Infrared LED marker for target recognition in indoor and outdoor applications of optical wireless power transmission system. *Jpn. J. Appl. Phys.* **2020**, *59*, SOOD06. [CrossRef]
24. Zhang, S.; Hu, G.; Wang, L.; Liu, Y.; Wei, L.; Zheng, Y.; Shao, Y. Wireless laser power transmission system for dynamic target using rotation of single component. *Laser Optoelectron. Prog.* **2022**, *59*, 1736001. [CrossRef]
25. William Setiawan Putra, A.; Kato, H.; Adinanta, H.; Maruyama, T. Optical wireless power transmission to moving object using Galvano mirror. In Proceedings of the SPIE, San Francisco, CA, USA, 1–6 February 2020; p. 11272. [CrossRef]
26. Zhou, W.; Jin, K. Optimal photovoltaic array configuration under Gaussian laser beam condition for wireless power transmission. *IEEE Trans. Power Electron.* **2017**, *32*, 3662–3672. [CrossRef]
27. Takeda, K.; Kawashima, N. Laser energy transmission to a disaster data collection helicopter. *Aerosp. Technol. Jpn.* **2012**, *11*, 57–60. [CrossRef]
28. Achtelik, M.C.; Stumpf, J.; Gurdan, D.; Doth, K.M. Design of a flexible high-performance quadcopter platform breaking the MAV endurance record with laser power beaming. In Proceedings of the IEEE/RSJ International Conference on Intelligent Robots and Systems, San Francisco, CA, USA, 25–30 September 2011; pp. 5166–5172. [CrossRef]
29. Laser-Powered Quadrocopter Endurance Demonstration by LaserMotive. Available online: https://www.youtube.com/watch?v=8hhv9Cu98us (accessed on 14 December 2024).
30. Sprangle, P.; Hafizi, B.; Ting, A.; Fischer, R. High-power lasers for directed-energy applications. *Appl. Opt.* **2015**, *54*, 201–209. [CrossRef] [PubMed]
31. Intelligent Drones That Never Land! A New Breakthrough in Optics-Driven Drone Research at WSU! (Chinese). Northwestern Polytechnical University. Available online: https://m.cyol.com/gb/articles/2022-12/30/content_gGw7nbHlqV.html (accessed on 14 December 2024).
32. Lim, Y.; Choi, Y.W.; Ryoo, J. Study on laser-powered aerial vehicle: Prolong flying time using 976 nm laser source. In Proceedings of the International Conference on Information and Communication Technology Convergence, Jeju Island, Republic of Korea, 20–22 October 2021; pp. 1220–1225. [CrossRef]
33. Bauersfeld, L.; Scaramuzza, D. Range, endurance, and optimal speed estimates for multicopters. *IEEE Robot. Autom. Lett.* **2022**, *7*, 2953–2960. [CrossRef]
34. Subudh, B.; Pradhan, R. A comparative study on maximum power point tracking techniques for photovoltaic power systems. *IEEE Trans. Sustain. Energy* **2012**, *4*, 1. [CrossRef]
35. Lee, S.; Lim, N.; Choi, W.; Lee, Y.; Baek, J.; Park, J. Study on battery charging converter for MPPT control of laser wireless power transmission system. *Electronics* **2020**, *9*, 1745. [CrossRef]
36. Tang, J.; Matsunaga, K.; Miyamoto, T. Numerical analysis of power generation characteristics in beam irradiation control of indoor OWPT system. *Opt. Rev.* **2020**, *27*, 170–176. [CrossRef]
37. Shen, C.; Ling, X.; Li, Y.; Chen, S.; Deng, Y. Practical efficiency limit of laser power converters based on lead halide perovskite. *Appl. Phys. Lett.* **2023**, *123*, 153301. [CrossRef]
38. Miyamoto, T.; Ueda, K.; Zhang, J.; Tsuruta, K. Optical wireless power transmission technology for indoor equipment and mobilities. *Rev. Laser Eng.* **2023**, *51*, 122–128.
39. Xiao, Y.; Wang, J.; Liu, H.; Miao, P.; Gou, Y.; Zhang, Z.; Deng, G.; Zhou, S. Multi-junction cascaded vertical-cavity surface-emitting laser with a high power conversion efficiency of 74%. *Light Sci. Appl.* **2024**, *13*, 60. [CrossRef] [PubMed]
40. Helmers, H.; Lopez, E.; Höhn, O.; Lackner, D.; Schön, J.; Schauerte, M.; Schachtner, M.; Dimroth, F.; Andreas Bett, A.W. 68.9% efficient GaAs-based photonic power conversion enabled by photon recycling and optical resonance. *Phys. Status Solidi* **2021**, *15*, 2100113. [CrossRef]